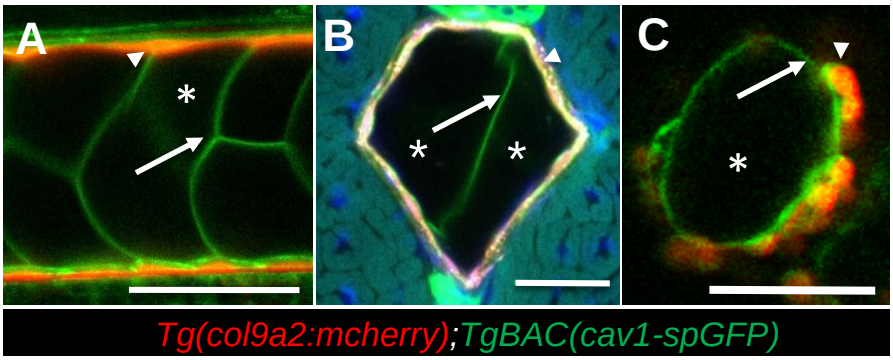
A
B
C
Tg(col9a2:mcherry);TgBAC(cav1-spGFP)

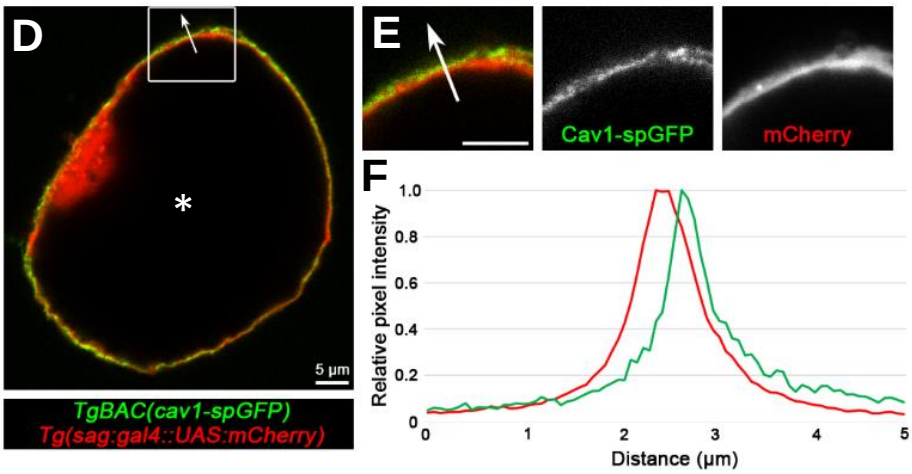
D
5 µm
TgBAC(cav1-spGFP)
Tg(sag:gal4::UAS:mCherry)
E
Cav1-spGFP
mCherry
F
Relative pixel intensity
Distance (µm)

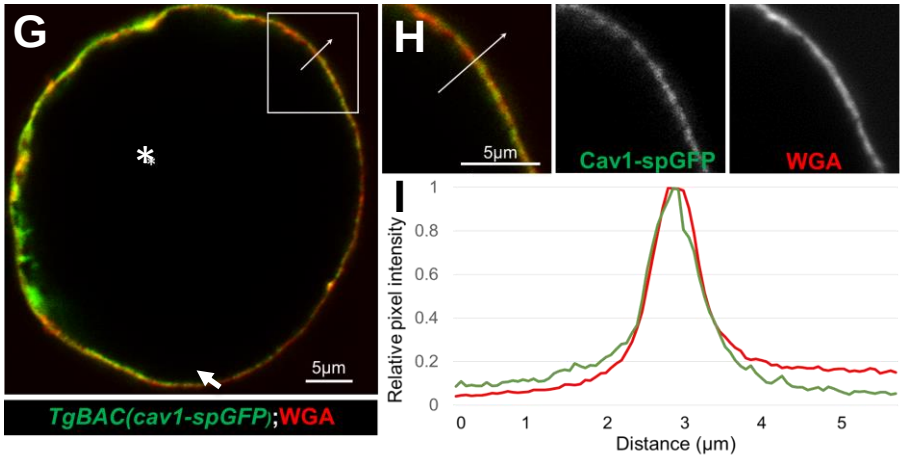
G
5µm
TgBAC(cav1-spGFP);WGA
H
5µm
Cav1-spGFP
WGA
I
Relative pixel intensity
Distance (µm)

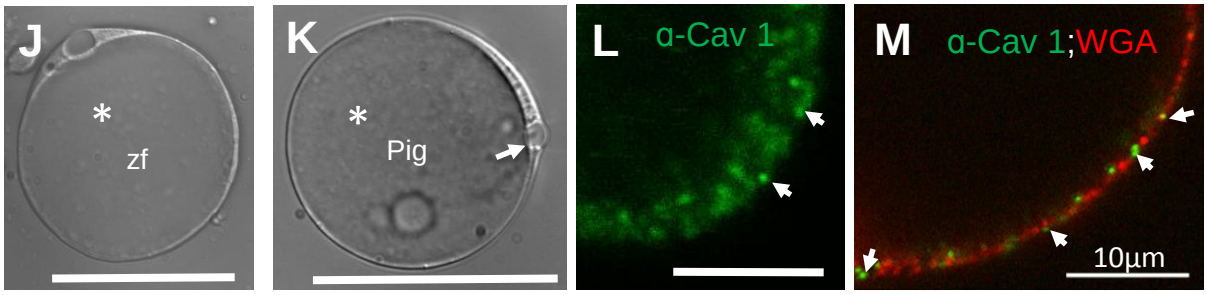
J
zf
K
Pig
L
α-Cav 1
M
α-Cav 1;WGA
10µm

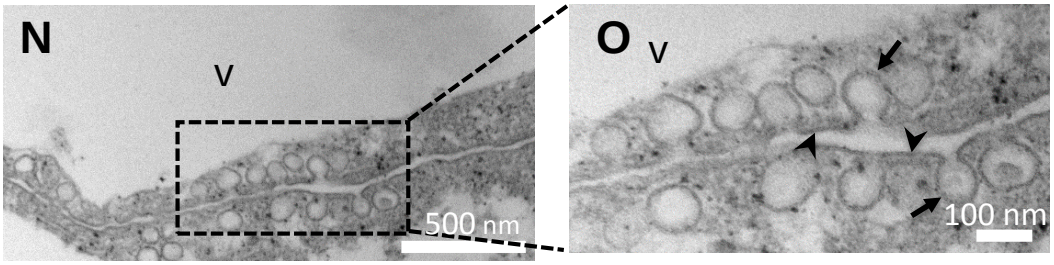
N
V
500 nm
O
V
100 nm

Figure S1. Caveolin 1 is a conserved vacuolated cell membrane protein in the vertebrate notochord. Related to Figure 1. A-C: Confocal images of a 72 hpf larva expressing *col9a2:mcherry, BAC(cav1-spGFP)*. **A:** Live image. Arrows point to vacuolated cell membranes, asterisks mark vacuole lumen. **B:** Cross section. Arrows point to vacuolated cell membranes, asterisks mark vacuole lumen. **C:** Live image of a partially dissociated notochord showing that Cav1-GFP is expressed in both vacuolated and sheath cells. Arrowhead points to a sheath cell. **D-F:** Live image of a vacuolated cell isolated from a 48 hpf zebrafish embryo expressing *BAC(cav1-spGFP)* and *sag:Gal4; UAS:mcherry-NTR;.* Cav1-spGFP exhibits a punctate pattern that is separated from the cytoplasmic mcherry signal as shown by a line scan (**F**) along the arrow. **G-I**: Live image of a vacuolated cell isolated from a 48 hpf zebrafish embryo expressing *BAC(cav1-spGFP)* and stained with Alexa-594 WGA to label cell surface glycans. Cav1-spGFP exhibits a punctate pattern at the plasma membrane similar to that of WGA as shown by a line scan (**I**) along the arrow. **J:** DIC image of a vacuolated cell isolated from a 72 hpf zebrafish larva. Scale bar 50μm. **K:** DIC image of a vacuolated cell isolated from the nucleus pulposus (NP) of a 6 months old pig. Scale bar 50μm. **L:** Thick optical section confocal image of a portion of a pig vacuolated cell stained for Cav1. The antibody labels punctae at the cell surface. Arrows point to plasma membrane Cav1+ punctae. Scale bar: 5μm. **M:** Thin optical section confocal image of a portion of a pig vacuolated cell stained for Cav1 and WGA. **N-O:** Transmission electron micrographs of NP issue. Abundant caveolae (arrows) are present at the plasma membrane (arrow heads) in two neighboring cells. V marks a vacuole.

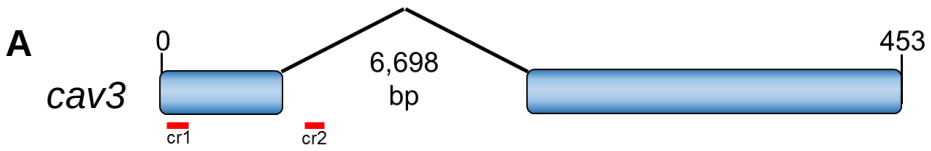
A
cav3
0
6,698
bp
453
cr1
cr2

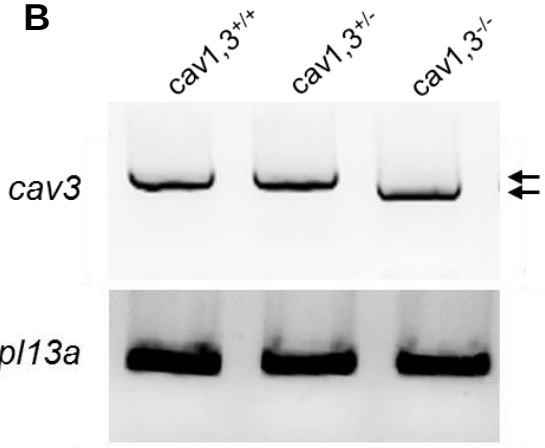
B
cav1,3+/+
cav1,3+/-
cav1,3-/-
cav3
rpl13a

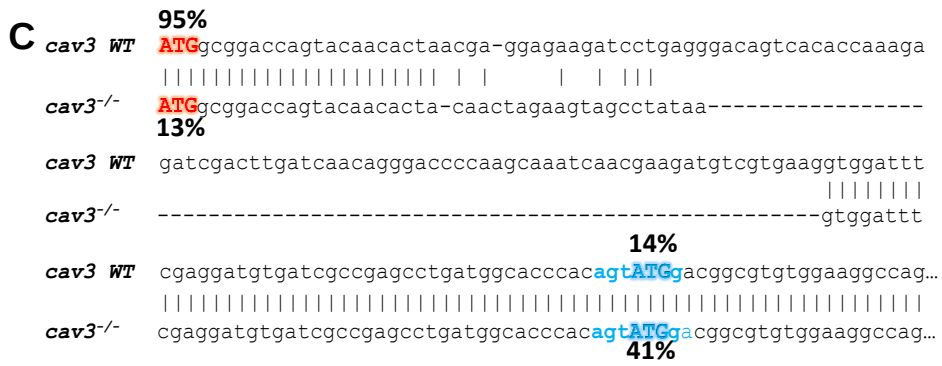
C
95%
cav3 WT ATGgcggaccagtacaacactaacga-ggagaagatcctgagggacagtcacaccaaaga
cav3-/- ATGgcggaccagtacaacacta-caactagaagtagcctataa----------
13%
cav3 WT gatcgacttgatcaacagggaccccaagcaaatcaacgaagatgtcgtgaaggtggattt
cav3-/- ----------gtggattt
14%
cav3 WT cgaggatgtgatcgccgagcctgatggcacccacagtATGgacggcgtgtggaaggccag…
cav3-/- cgaggatgtgatcgccgagcctgatggcacccacagtATGgacggcgtgtggaaggccag…
41%

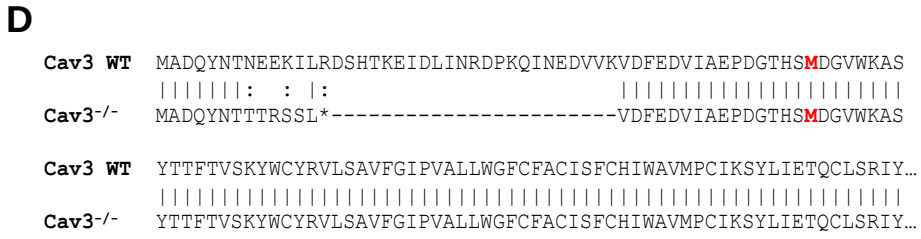
D
Cav3 WT MADQYNTNEEKILRDSHTKEIDLINRDPKQINEDVVKVDFEDVIAEPDGTHSMDGVWKAS
Cav3-/- MADQYNTTTRSSL*----------VDFEDVIAEPDGTHSMDGVWKAS
Cav3 WT YTTFTVSKYWCYRVLSAVFGIPVALLWGFCFACISFCHIWAVMPCIKSYLIETQCLSRIY…
Cav3-/- YTTFTVSKYWCYRVLSAVFGIPVALLWGFCFACISFCHIWAVMPCIKSYLIETQCLSRIY…

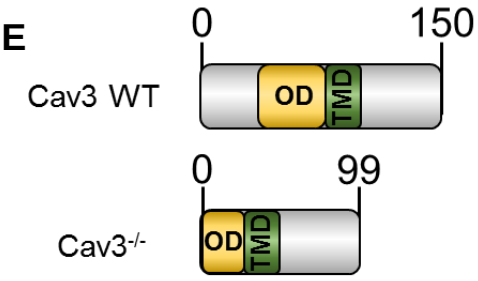
E
Cav3 WT
0
150
OD
TMD
Cav3-/-
0
99
OD
TMD

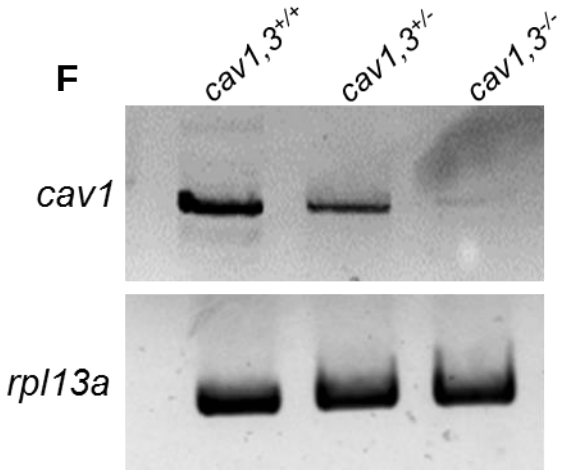
F
cav1,3+/+
cav1,3+/-
cav1,3-/-
cav1
rpl13a

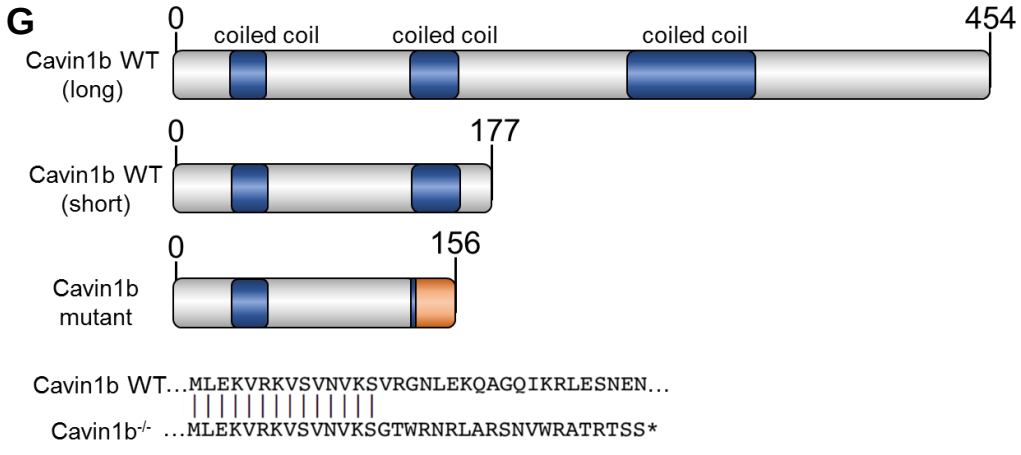
G
Cavin1b WT (long)
0
coiled coil
coiled coil
coiled coil
454
Cavin1b WT (short)
0
177
Cavin1b mutant
0
156
Cavin1b WT…MLEKVRKVSVNVKSVRGNLEKQAGQIKRLESNEN…
Cavin1b-/- …MLEKVRKVSVNVKSGTWRNRLARSNVWRATRTSS*

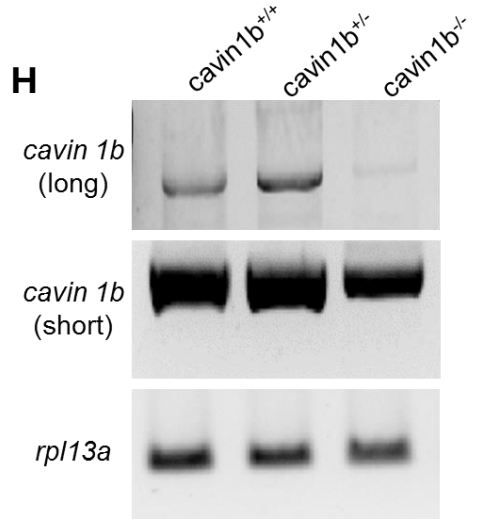
H
cavin1b+/+
cavin1b+/-
cavin1b-/-
cavin 1b (long)
cavin 1b (short)
rpl13a

Figure S2. Generation and molecular characterization of *cav3* and *cavin1b* mutants. Related to Figure 1 and 2. A: Generation of *cav3*^{pd1149} allele. Two guide RNAs were injected simultaneously to delete a genomic region spanning most of exon one and part of the first intron. **B:** RT-PCR using primers pairing in the 5' and 3' UTR of cav3 revealed that the *cav3*^{pd1149} is spliced to produce a slightly shorter transcript. WT and mutant transcripts are marked by arrows *rpl13a* was used as standard. **C:** cDNA sequence of WT and *cav3*^{pd1149} mutant transcripts. The % next to each ATG codon indicates the probability of functioning as a start site. The Kozac sequence of the alternative start site is indicated in blue. **D:** Predicted protein sequence produced by the WT and *cav3*^{pd1149} mutant transcripts. The genomic deletion creates an early stop codon and a deletion of part of the N-terminus in the mutant. The alternative first aa is indicated in bold. **E:** Domain structure of WT and mutant Cav3. The N-terminus and part of the oligomerization domain (OD) are eliminated, leaving the trans-membrane domain (TMD) and the C-terminus intact. **F:** RT-PCR of α/β *cav1*. Both *cav1* transcripts largely decay in *cav1, 3* mutants. *rpl13a* was used as standard. **G:** Domain structure of Cavin1b showing the isoforms corresponding to the long and short transcripts and the predicted mutated protein. The mutation affects both transcripts and generated an early stop codon after a short stretch of missense sequence. **H:** RT-PCR showed that in *cavin1b* mutants the long transcript decays, whereas the short transcript still persists in the mutants. *rpl13a* was used as standard.

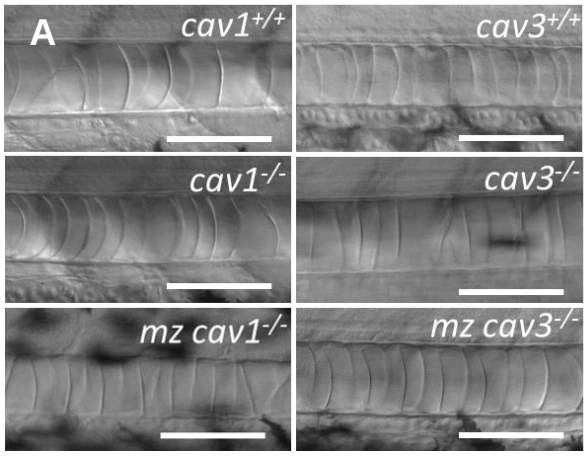

B

cross	Penetrance			
	cav1,3$^{+/-}$ * *cav1,3*$^{+/-}$	*mz cav1,3*$^{-/-}$	*cavin1b*$^{+/-}$ *cavin1b*$^{+/-}$	*mz cavin1b*$^{-/-}$
72hpf	4.23%	78%	14.90%	96.40%
96hpf	8.08%	82%	24.70%	99.70%
n=	260	119	194	279

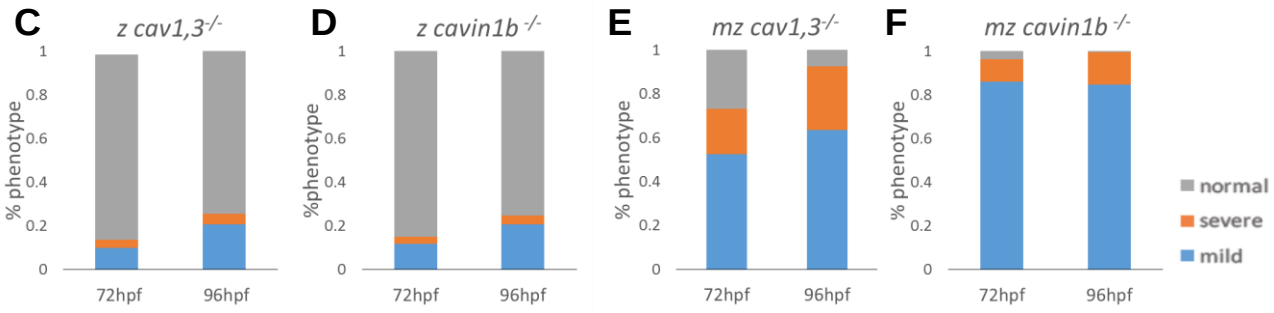

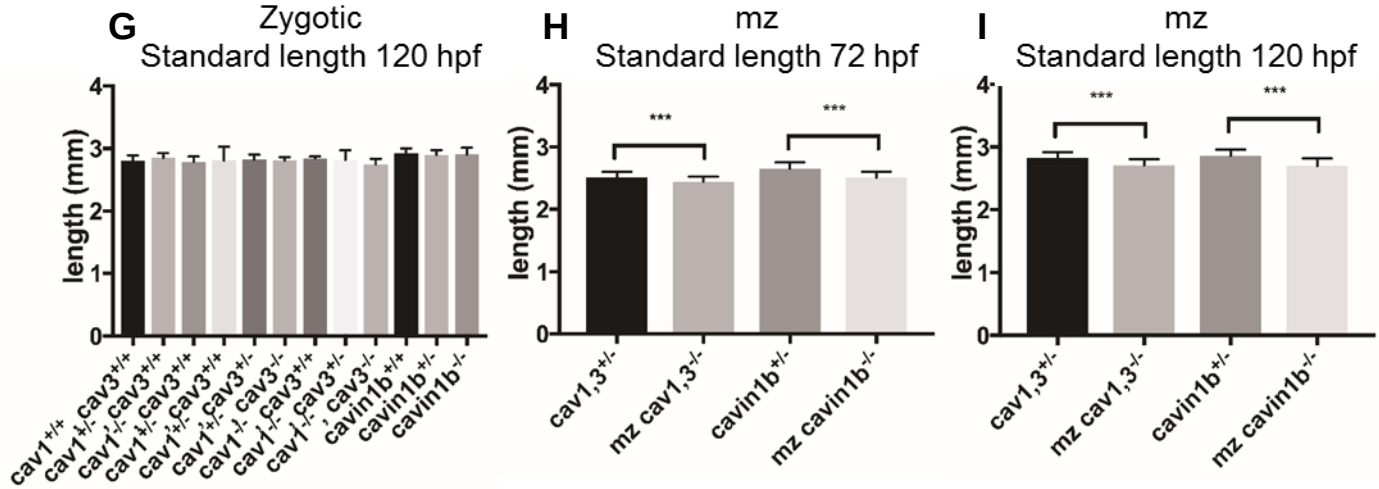

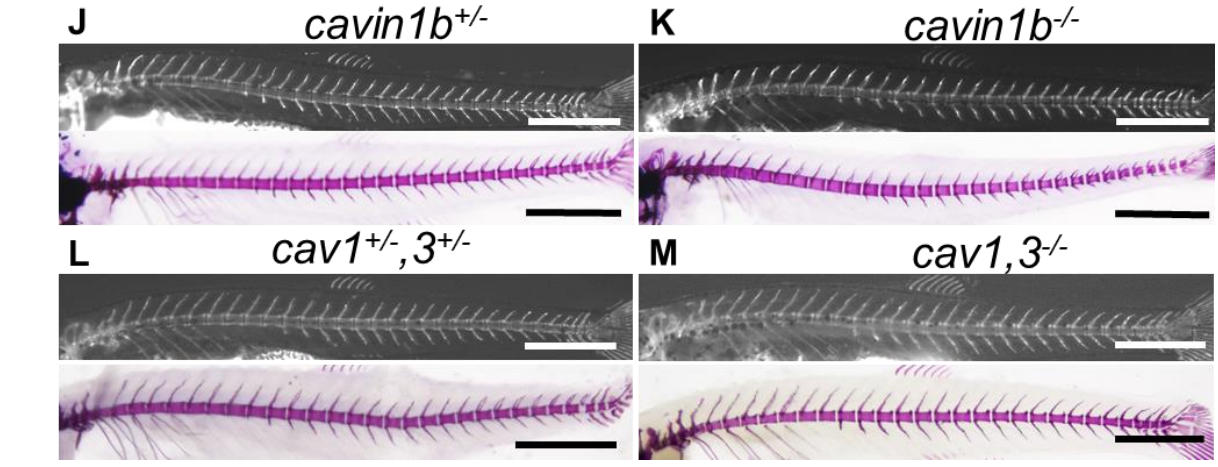

Figure S3. Phenotypic characterization of caveolar mutants. **Related to Figure 1, 2, 3 and 4. A**: DIC images of notochords of 72 hpf WT and zygotic or maternal zygotic (mz) *cav1*$^{-/-}$, or zygotic and mz *cavin1b*$^{-/-}$. No anatomical or notochord phenotypes were observed. Scale bars=100µm . **B:** Analysis of penetrance for zygotic or mz mutants. Values correspond to fraction of the fish with notochord phenotype. * Note that for the *cav1,3*$^{+/-}$ cross the penetrance at 96 hpf is higher than expected due to the fact that up to 87% of *cav3*$^{-/-}$, *cav1*$^{+/-}$ larvae present notochord phenotype. **C-F:** Analysis of severity of notochord phenotype in zygotic and mz *cav1, 3* and *cavin1b* mutants. Fish were scored as indicated (Fig 1L). n=260, 194, 82, and 279 respectively. **G:** Body length measurements of genotyped 120 hpf larvae from *cav1,3*$^{+/-}$ and *cavin1b*$^{+/-}$ in-crosses. No significant differences were detected. One-way ANOVA, Tukey's test, *p*=0.29, n=13, 54, 46, 48, 151, 117, 117, 11, 53, 47, 56, 94, 41 respectively **H-I:** Body length measurements of 72 and 120 hpf mz *cav1, 3*$^{-/-}$, *cavin1b*$^{-/-}$ and *cav1,3*$^{+/-}$ and *cavin1b*$^{+/-}$. Due to the slightly earlier onset of the notochord phenotype respect to zygotic mutants, mz mutants show a small but significant reduction in body length compared to heterozygous fish. One-way ANOVA with Tukey's test, ***p<0.001, n=83, 81, 73, 70, 74, 81, 73, 70 respectively. **J-K:** Live calcein staining (top panel) and alizarin red skeletal preparations (bottom panel) of WT and mz *cavin1b*$^{-/-}$ mutant fish. No spine defects were detected (n=19 mutants). Scale bars=1mm .**L-M:** Live calcein staining (top panel) and alizarin red skeletal preparations (bottom panel) of WT and mz *cav1, 3*$^{-/-}$. No spine defects were detected (n=26 mutants). Scale bars=1mm.

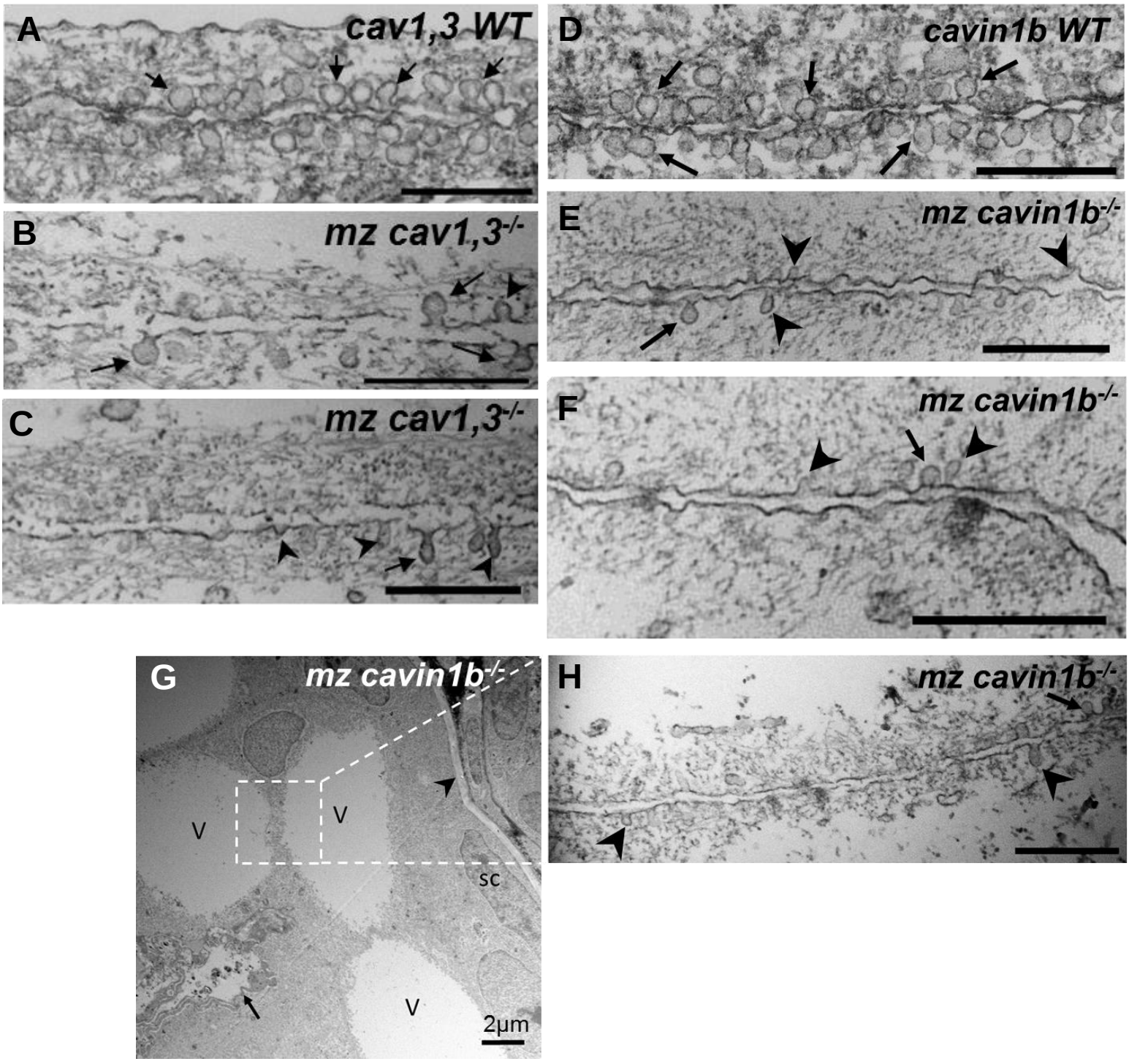
A
cav1,3 WT
B
mz cav1,3-/-
C
mz cav1,3-/-
D
cavin1b WT
E
mz cavin1b-/-
F
mz cavin1b-/-
G
mz cavin1b-/-
V
V
sc
V
2µm
H
mz cavin1b-/-

Figure S4. Ultrastructural analyses of caveolar mutants. **Related to Figure 1, 2, 3 and 4.** **A-C:** Transmission electron microscopy (TEM) images of 72 hpf WT and mz *cav1, 3*$^{-/-}$ larvae taken from areas of the inner notochord where two vacuolated cells meet. In WT we detected an average of 6 caveoalae per µm of plasma membrane, whereas there were only 1/µm in mz *cav1, 3*$^{-/-}$ larvae. Arrows point to omega shaped caveolae and arrowheads point to dysmorphic caveolae. **D-F:** TEM images of 72 hpf WT and mz *cavin1b*$^{-/-}$ larvae taken from areas of the inner notochord where two vacuolated cells meet. In WT we detected an average of 6.8 caveoalae per µm of plasma membrane, whereas there were only 1.5/µm in mz *cavin1b*$^{-/-}$ larvae. Arrows point to omega shaped caveolae and arrowheads point to dysmorphic caveolae. **G:** Low magnification TEM image of a mz *cavin1b*$^{-/-}$ larvae with a severe notochord lesion. Several newly vacuolated cells, marked V, were found next to the remnants of a collapsed primary vacuolated cell, marked with an arrow (see also Fig. 2D and Fig. 4). The arrowhead marks the matrix around the sheath, sc=sheath cell. **H:** TEM image of an area were to newly vacuolated cells meet. As shown for primary vacuolated cells, few caveolae are found at the plasma membrane (arrow) and dysmorphic caveolae (arrowheads) are also present. Scales bars are 500 nm.